Electrokinetics coupling with microbially-induced calcite precipitation that strengthens the chromate removal in the bio-electrochemical system

Tao Huang[a,b,c,*], Longfei Liu[a], Shuwen Zhang[d]

[a]*School of Chemistry and Materials Engineering, Changshu Institute of Technology, No. 99, South 3rd Ring Road, Changshu 215500, China, emails: ht1104705720@qq.com (T. Huang), longfeiliu_cslg@163.com (L. Liu)*
[b]*Suzhou Key Laboratory of Functional Ceramic Materials, Changshu Institute of Technology, Changshu 215500, China*
[c]*School of Chemical and Technology, China University of Mining and Technology, Xuzhou 221116, China*
[d]*Nuclear Resources Engineering College, University of South China, Hengyang 421001, China, email: tillg14536@yahoo.com*

ABSTRACT

Hexavalent chromium (Cr(VI)) is a well-known carcinogen, which must be completely removed from the contaminated water or reduced to a less toxic state. In this work, a bio-electrochemical platform combining electrokinetics (EK) and microbially induced calcite precipitation (MICP) was assembled to enhance Cr(VI) removal from the stocking solution. The chromate was removed mainly by the chemical precipitation of $CaCrO_4$ and further immobilized by $CaCO_3$ produced from the microbial bio-mineralization in the bioremediation. The coupling method was proved to be more effective in increasing the removal efficiencies of Cr(VI) and enhancing the immobilization of Cr(VI) compared with using bioremediation or electrokinetics alone. The maximum efficiency of 97.63% was achieved in the bio-electrochemical experiments. The exchangeable fraction of Cr(VI) was significantly reduced from 40.12% to 22.34% in the precipitation obtained from the bio-electrochemical system. A relatively high voltage was preferred in the coupling system. Generally, the combination of EK and MICP not only strengthened the removal of Cr(VI) from the solution and also significantly reduced the potential re-release of Cr(VI) in the final precipitation.

Keywords: Electrokinetics; Microbially induced calcite precipitation; Bio-electrochemical; Bio-mineralization; Chromate removal

1. Introduction

Chromium (Cr) is released into the aqueous environment through both geogenic and anthropogenic activities. The valence of chromium ranges from −2 (the lowest) to +6 (the highest), with the hexavalent chromium being of most obvious environmental toxicity [1]. Cr(VI) having carcinogenic and mutagenic effects on the human tissues and organisms is classified as a Class-A carcinogen by the US Environmental Protection Agency [2,3]. The symptoms including skin-inflammation, severe ulcer, kidney damage, and pulmonary congestion, etc., are also related to Cr poisoning or Cr enrichment in the blood vessels [4]. Most of the Cr slag-producing industry illegally discharge polluted solid waste (e.g., slag, unprocessed residue, and chemical byproduct) to the surrounding environment due to the inadequate investment of disposal facilities in China, which has caused the frequent occurrence of the serious pollution accidents in the local villages [5]. The upper limit of Cr is capped under 0.05 mg/L in the drinking water conforming to the standard (WHO, 1993) of the World Health Organization [2,6,7]. Cr(VI) must be significantly separated

* Corresponding author.

from the industrially polluted water or reduced to a less toxic state before the wastewater getting released into the ecosystem.

The treatment and remediation of Cr-contaminated wastewater are mainly relying on the application of the traditional physicochemical techniques, such as evaporation, reverse osmosis, membrane filtration, oxidation/reduction, methylation/demethylation, coagulation/flocculation, chemical precipitation, and electrochemical treatment [8–12]. The technology of chemical precipitation has been widely used to remove heavy metals (HMs) from wastewater [13]. However, the fluctuation of the precipitating agents such as calcium hydroxide and calcium magnesium carbonate in price and the high instability of precipitation have limited the further industrial promotion in processing the Cr-contaminated wastewater on a large scale. The other physicochemical techniques for remediating the wastewater not only have the high requirement of energy cost, chemical reagents, and specific equipment, also inevitably generate secondary contaminants [14–17]. Generally, the traditional physicochemical methods are not well appropriate in efficiently removing Cr(VI) from the wastewater based on the environmental mobility and chemical speciation of Cr.

Bioremediation of Cr(VI) has been considered to be more environmentally friendly and cost-effective by using microbes as an eco-compatible approach [14,18]. The microbially induced calcite precipitation (MICP) is proved to be efficacious in immobilizing the anions and cations of HMs in the carbonate fraction based on the participation of ureolytic bacteria [19,20]. Calcite is assembled through the octahedral CaO_6 corner-sharing with triangular groups of CO_3, making it capable of accommodating a wide range of substituent ions. The mobility of Cr(VI) can be affected by the incorporation (Co-precipitation) or the substitution (biomineralization) of CrO_4^{2-} to the structure of the calcite [20,21]. The immobilization of Cr(VI) on the calcareous skeleton from the aqueous environment is comprehensively influenced by the solution concentration of Cr(VI), type of the calcite, and the availability of surface sites [21,22]. Considering the co-precipitation of chromate oxyanion is relatively weak (i.e., which is sensitive to the acidification), and the substitution kinetics of CrO_4^{2-} is much lower than the pure cations, the strengthening measurements must be chosen to overcome the drawbacks of MICP. The high microbial sensitivity to the living environment (e.g., redox potential, oxygen dissolution, and metal toxicity) is also needed to be considered when conducts the enhancing step.

Electrokinetics (EK) has attracted strong interest as an effective tool to remediate the heavy-metal-contaminated fine-grained soils [23–25]. The remediation target is primarily achieved by electromigration, electroosmosis, and water decomposition [23–26]. In the work, a bio-electrochemical platform was assembled to implement the experiments. EK and MICP are employed in combination to enhance Cr(VI) removal from the stocking solution. The biological characteristics including bacterial growth, urease production, and ureolytic activity of the isolated bacterial (i.e., from the chromium slag) were investigated under the different concentrations of Cr(VI) oxyanions and urea. An orthogonal test with four factors with four levels was designed to study the effects of the voltage gradient,

remediation time, initial pH, and Ca^{2+} concentration on the bacterial growth, the precipitation of calcium carbonate (i.e., $CaCO_3$), and the removal efficiency of Cr(VI), and to quantitatively determine the optimal combination of operating parameters based on the analysis of significance probability and marginal means. A suitable kinetic model was further constructed in the optimal condition to predict Cr(VI) concentration in the electrolyzer over time. A five-step sequential extraction procedure (Tessier extraction) was used to evaluate the potential release characteristics of Cr(VI) from precipitations to further testify the EK influence on MICP [27,28]. The study proposes a novel method in further increasing the removal rate of Cr(VI) from industrial wastewater and solving one of the intrinsic issues of bioremediation, the potential contamination of sludge production.

2. Methods and materials

The chemicals and reagents used in this study are specifically listed in the supporting information (Chemicals, and regents). All the chemicals and reagents were sterilized before usage. The urease-producing bacterium, *Bacillus* sp.H1 (gram-positive) used in this research was previously isolated from a puddle of the chromium slag, in China [29]. The isolation and activation of ureolytic bacteria are provided in the SI. The specifications of three media including the urease-selective (URS), Luria–Bertani, and the nutrient broth (NB) are detailed in Tables S1–S3. A cylindrically electrokinetic electrolyzer (Φ 10 cm, height 10 cm) was constructed to study the effect of EK on the bioremediation process. The schematic diagram of the reactor is shown in Fig. 1. A graphite rod (Φ 2 cm, height 8 cm) acting as
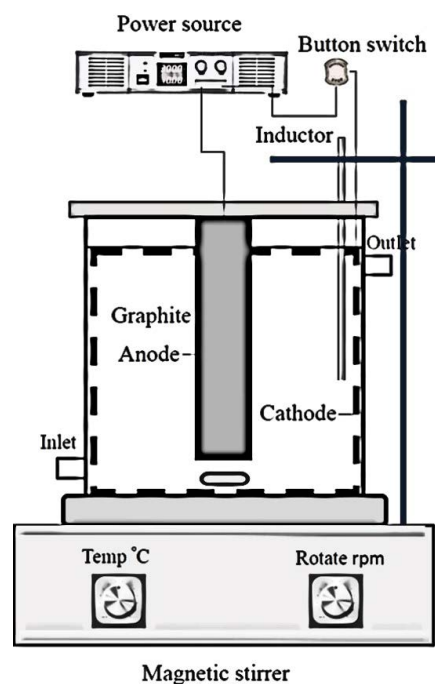

Fig. 1. Schematic diagram of the bio-electrochemical reactor.

the anode was embedded in the central axis of the single chamber. The carbon cloth (monolayer) chosen as the cathode was attached around the cylindrical shell. A direct-current power source (E3632A, KEYSIGHT) was connected to the bio-electrochemical platform to supply the constant voltage. 500 mL of NB medium loaded with 50 g/L urea, 50 μmol/L Ni²⁺, 0.05 M CaCl₂, and 120 mg/L K₂Cr₂O₇ was added to the reactor, magnetically stirred at 150 rpm, and maintained by a heating bar at 25°C. A two-factor group (16 runs) and an orthogonal system (16 runs) were synchronously implemented to straightly demonstrate the coupling effect of the enhancing experiments. The detailed information on the factors and levels is listed in Table S4. The two-factor experiments at four different levels were constructed to study the effect of the initial pH and Ca²⁺ concentration on the pure bioremediation process in Table S5. The orthogonal tests $L_{16}(4^5)$ with four factors at four different levels were designed to study the effect of the voltage gradient (V/cm), the remediation time (d), initial pH, and Ca²⁺ concentration (M) on the removal efficiency (R-e, %) during the EK-MICP process (Table 1). A bacteria-free group was set as the control under the same orthogonal condition to analyze the influence of single EK on the Cr(VI) removal (R-e$_{free}$, %).

The supernatants were extracted using a sterilized glass pipette (2 mL) from each group during the experiments. Cr(VI) in the solution was measured using a UV-visible spectrophotometer (DR6000, HACH, USA) at 540 nm (GB/T15555.4–1995, diphenylcarbazide method). The concentration of calcium ion was determined by inductively coupled plasma optical emission spectroscopy (ICP-OES; iCAP™ 7600, Thermo Fisher Scientific, USA). The chemical speciation of the final precipitation obtained through both single MICP (bioremediation) and EK-MICP (bio-electrochemical) method was analyzed using the five-stage Tessier sequential extraction procedure (Fig. S1). The experimental data including R-e and R-e$_{free}$ recorded from the two-factor and orthogonal tests were quantitatively analyzed by the analysis of variance (ANOVA). The marginal means (MM) were evaluated by Tukey's test ($p < 0.05$, default α = 0.05) using IBM SPSS software (edition: 20). R-e or R-e$_{free}$ is calculated following Eq. (1), where $c_{Cr}(0)$ is the initial concentration (mg/L) of Cr(VI), and $c_{Cr}(t)$ represents Cr(VI) concentration (mg/L) at time t. The precipitation efficiency (P-e) of Ca²⁺ was calculated using Eq. (2), where $c_{Ca}(0)$ is the initial concentration (M) of Ca²⁺, and $c_{Ca}(t)$ is Ca²⁺ concentration (M) at time t. Three known kinetic models including the pseudo-first-order model, pseudo-second-order model, and Elovich were modified to simulate Cr(VI) removal overtime in the bioremediation and bio-electrochemical experiments. The three kinetic models are detailed in the supporting information (Eqs. (S1)–(S3)).

$$R\text{-e}\left(\text{or } R\text{-e}_{free}\right) = \left(1 - \frac{c_{Cr}(t)}{c_{Cr}(0)}\right) \times 100\% \tag{1}$$

$$P\text{-e} = \left(1 - \frac{c_{Ca}(t)}{c_{Ca}(0)}\right) \times 100\% \tag{2}$$

3. Results and discussions

3.1. Urease production and bacterial growth

The plates with the urease-selective medium (Table S1) were changed in the color after 2 d incubation, from the initial pale orange to a darker pink. The color of the urea-free group has no obvious change in comparison. The macro

Table 1
Design of orthogonal tests for the bio-electrochemical system (four factors with four levels, ($L_{16}(4^5)$))

Test no.	A^a	B^b	C^c	D^d	R-e	R-e$_{free}$
1	1 (0.1 V/cm)	1 (3 d)	1 (7)	1 (0.05 M)	59.27%	5.52%
2	3 (1.0 V/cm)	3 (9 d)	1	3 (0.15 M)	93.31%	31.17%
3	4 (1.5 V/cm)	4 (12 d)	1	4 (0.20 M)	97.63%	36.78%
4	2 (0.5 V/cm)	2 (6 d)	1	2 (0.10 M)	73.52%	24.13%
5	2	4	3 (9)	1	69.24%	30.18%
6	4	3	2 (8)	1	75.23%	33.27%
7	3	2	4 (10)	1	72.52%	26.49%
8	1	4	4	3	70.75%	13.21%
9	4	1	4	2	84.84%	19.94%
10	1	3	3	2	66.86%	11.47%
11	2	3	4	4	94.47%	27.74%
12	2	1	2	3	89.92%	15.55%
13	3	1	3	4	96.12%	17.42%
14	3	4	2	2	83.63%	34.45%
15	4	2	3	3	95.58%	28.76%
16	1	2	2	4	69.72%	8.22%

[a]Voltage gradient (V/cm); [b]remediation time (d); [c]initial pH; [d]Ca²⁺ concentration (M).

phenomenon directly demonstrated the production of urease by the microorganisms and reflected the potential effect of urea on the bacterial activity (i.e., Eq. (3)). The extra urea added to the culture of *Bacillus* sp.H1 would not only supply the nitrogen (N) element for the bacterial growth and also guarantee the production of precipitation inducer (i.e., CO_3^{2-}). However, the urea in the medium can inhibit bacterial activity on the contrary when its concentration has exceeded the adaptability of microorganisms. As shown in Fig. 2a, the growth curve of the control run (i.e., urea free) is consistent with the standard curve. The concentration of 40 g/L urea seemingly has no significant impact on the growth of bacteria. However, the further increase of urea concentration burdened the bacterial amplification in general. The activity of bacteria has been significantly restricted in the culture with 100 g/L urea. The *Bacillus* sp.H1 barely grew in the aqueous environment with a high concentration of urea (i.e., >100 g/L). 40–60 g/L of urea was recommended to be added to the medium, which guaranteed the growth and functionality of bacteria, and satisfied the necessary conditions for bio-mineralization. Cr(VI) is considered as a strong oxidizing agent, which can irreversibly destroy the DNA structure of microorganisms. The too high concentration of Cr(VI) also can cause the denaturation of protein and reduce the activity of metabolism-related enzymes. As shown in Fig. 2b, the *Bacillus* sp.H1 had a certain resistance to low concentrations of Cr(VI). The corresponding growth curves were broadly similar to that of the control group (i.e., Cr(VI) free). The four stages of bacterial growth had been hardly recognized when the concentration of Cr(VI) was elevated to 120 mg/L. The environment of the medium has become extremely harsh for bacterial growth when the concentration of Cr(VI) was further raised to 150 or 180 mg/L. Overall, the *Bacillus* sp.H1 cannot adapt well to the living environment by regulating its metabolism when it is exposed to Cr(VI) above 150 mg/L.
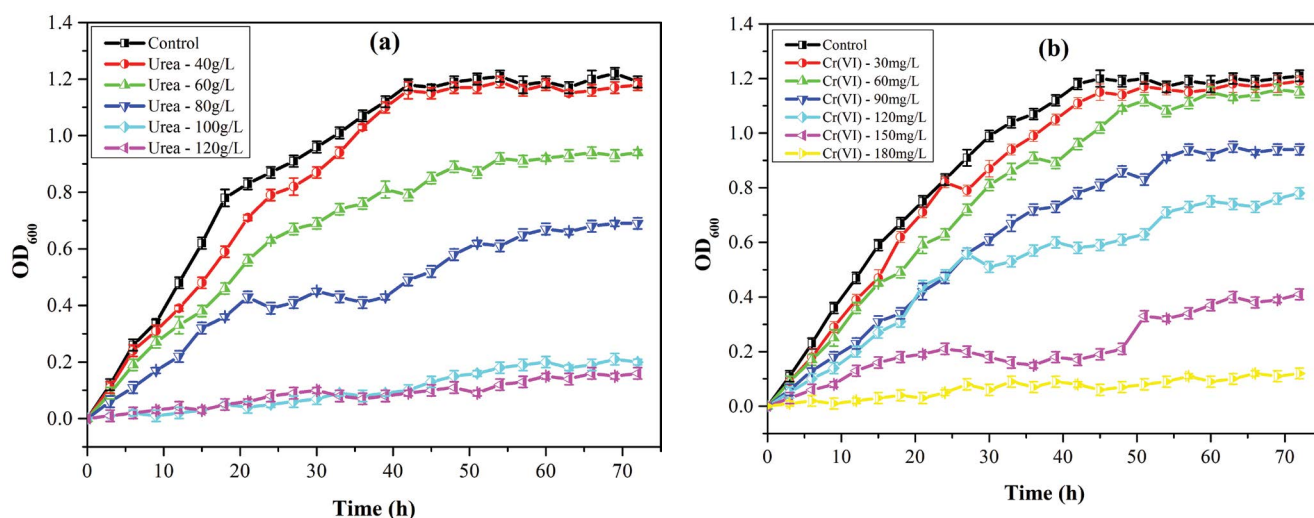
$$CO(NH_2)_2 + 2H_2O \xrightarrow{\text{Urease}} 2NH_4^+ + CO_3^{2-} \qquad (3)$$

3.2. Calcite precipitation in the MICP experiment

The organic carbon in the solution can be utilized by the MICP microorganisms for the bioactivities, and eventually transformed into inorganic carbon (i.e., carbonate). *Bacillus* genus bacteria categorized as "Gram-positive" bacteria, contains teichoic acids on the thick cell walls, which contributes to the negative charge of the cell wall. Ca^{2+} ions are electrostatically attracted to the cell wall, which further induces the relevant mineralization reactions (Eqs. (4) and (5)) at the sites of cell wall when the binding sites reach saturation for the ureolytic bacteria. As shown in Fig. 3a, 95.45%, 93.27%, and 85.54% precipitation efficiencies (P-e) of Ca^{2+} (0.05 M) were achieved in the group of 60, 90, and 120 mg/L, respectively. P-e was remarkably reduced when the concentration of Cr(VI) was increased to 150 mg/L. The results corresponded to the bacterial growth in the different concentrations of Cr(VI) (Fig. 2b), indicating the growth inhibition of the bacteria caused by the high concentration of Cr(VI) would further lower the distribution of calcium in the form of the bio-mineralization. Cr(VI) commonly forms outer-sphere complexes adsorbing on the mineral surfaces, can also substitute the carbonate in the calcite structure. Considering the toxicity of Cr(VI) to bacteria, the existence of Cr(VI) in medium imposes a potential effect on the process of precipitation or Cr-calcite co-precipitation. The effect of Cr(VI) concentration on the removal efficiencies (R-e) of Cr(VI) in the bioremediation process is displayed in Fig. 3b. The final R-e values gradually decreased with the increase of Cr(VI) concentration. The highest efficiency obtained in the group of 60 mg/L-Cr(VI) was 57.18% (deviation: ±1.5%). Contrarily, the final R-e value of Cr(VI) in the bacteria-free group of 60 mg/L-Cr(VI) was lowest, only 24.31% (deviation: ±1.5%). The non-biological moiety was mainly attributed to the generation of chemical precipitation $CaCrO_4$ (Eq. (6)). Generally, the P-e values were positively relevant with the R-e values in the medium compensating with different Cr(VI) concentrations, which indicated that the removal of Cr(VI) was controlled by both the calcite carbonates by microbial urease (i.e., bio-mineralization) and
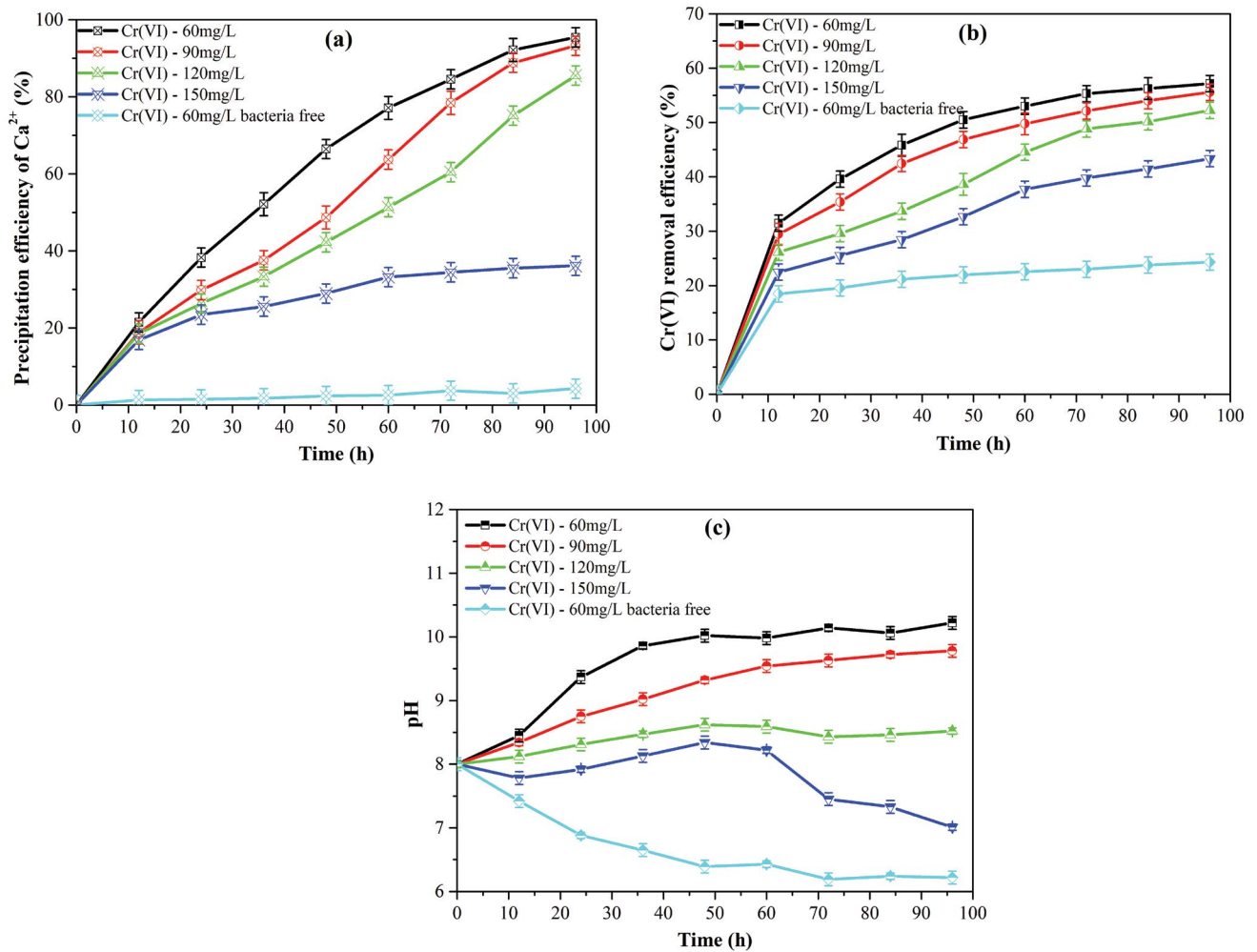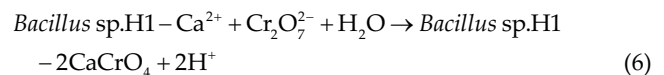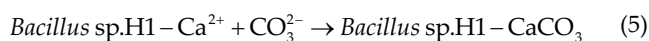
Fig. 2. Effect of the concentration of urea (a) and Cr(VI) (b) on the growth of bacteria (*Bacillus* sp.H1).

Fig. 3. Effect of the concentration of Cr(VI) on the precipitation efficiency of Ca^{2+} (a), the removal efficiency of Cr(VI) (b), and change of pH (c) in the MICP experiments.

the production of $CaCrO_4$. MICP is an ureolytically driven process, the hydrolysis of urea catalyzed by the bacterial urease increases the pH, facilitating the accumulation of M^{2+} ions and carbonate, and resulting in the mineral saturation at the active sites of the cell wall. The changes in pH over time in groups were recorded in Fig. 3c. As shown, the pH eventually deceased from the initial 8 to the final 6.22 (deviation: ±0.1) at 96th hour in the bacteria-free group (with 60 mg/L Cr(VI)). The dissolution of CO_2 in the medium from air and the generation of H^+ ions (Eq. (6)) were blamed on the result. Comparatively, the alkalinity in the two groups of 60 and 90 mg/L-Cr(VI) has been apparently increased, from the initial 8 to the final 10.22 (deviation: ±0.1) and 9.78 (deviation: ±0.1), respectively, which directly reflected the hydrolysis of urea and demonstrated the activity of the urease-producing bacteria in the solution with the relatively lower Cr(VI) concentration.

$$Bacillus\ sp.H1 + Ca^{2+} \rightarrow Bacillus\ sp.H1 - Ca^{2+} \tag{4}$$

$$Bacillus\ sp.H1 - Ca^{2+} + CO_3^{2-} \rightarrow Bacillus\ sp.H1 - CaCO_3 \tag{5}$$

$$\begin{aligned} Bacillus\ sp.H1 - Ca^{2+} + Cr_2O_7^{2-} + H_2O &\rightarrow Bacillus\ sp.H1 \\ - 2CaCrO_4 + 2H^+ \end{aligned} \tag{6}$$

3.3. Electrokinetic optimization

The removal results (R-e, %) of Cr(VI) in the two-factor experiments characterizing the pure bioremediation process are listed in Table S5. The corresponding significance-analysis results of the two variables are displayed in Table 2. The estimated marginal means of the removal efficiencies of Cr(VI) affected by each factor are shown in Fig. 4a. The maximum R-e was 73.36% (average value obtained in the triplicate), achieved at the initial pH of 10 (C4) and the concentration of Ca^{2+} of 0.20 M (D4). The adjusted R^2 equaled 0.961, indicating the significance analysis based on the two-factor experiments for the bioremediation process was highly reliable. The significance probabilities of the two variables (Table 2, i.e., 0.000 and 0.000) were both much less than the default α value of 0.05, which demonstrated that the change of the initial pH and the Ca^{2+}-concentration dosing in the medium both could
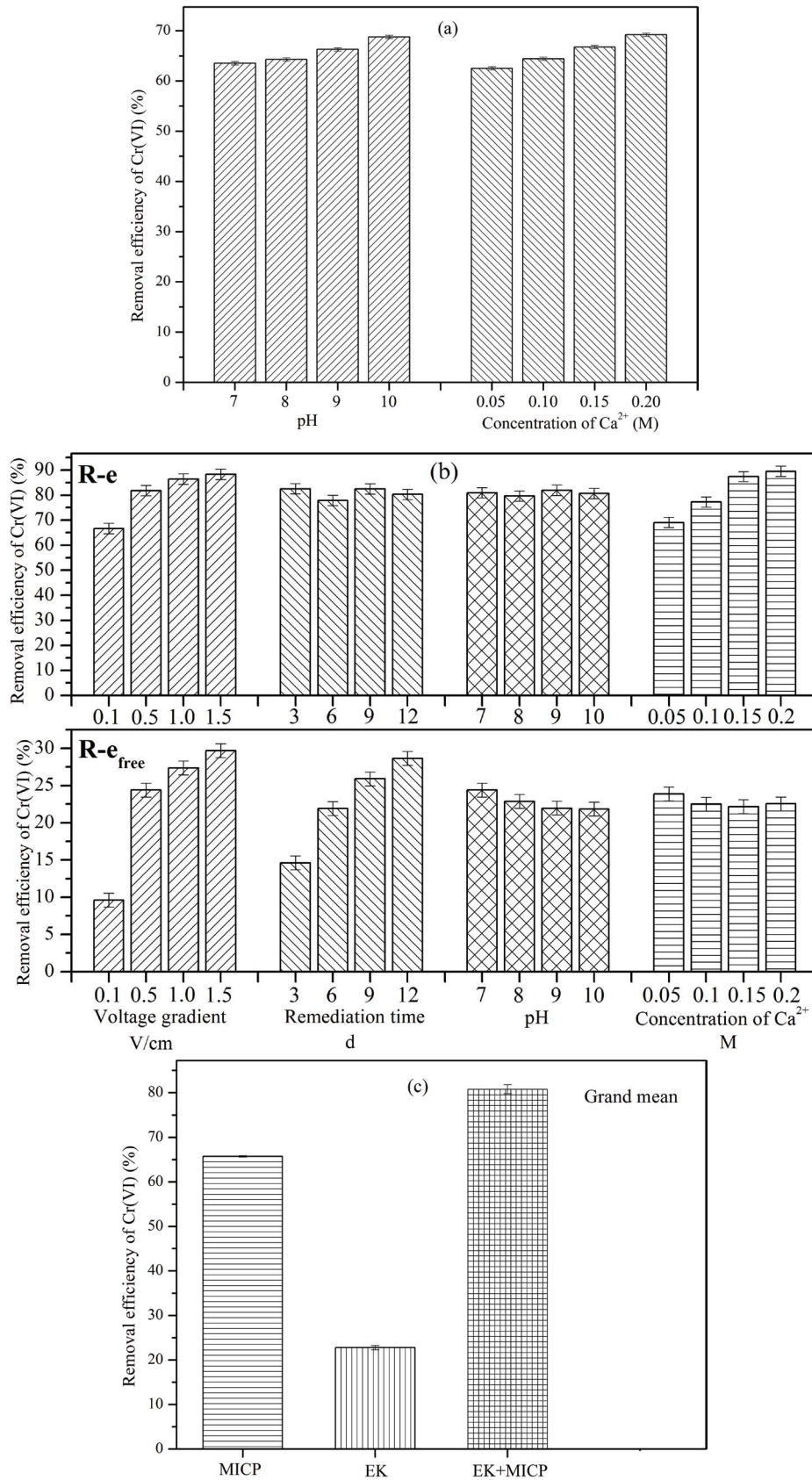
Fig. 4. Estimated marginal means governed by each factor in the pure bioremediation (a) and the bio-electrochemical system (b), and the grand means for the three remediation systems (c).

Table 2
Significance tests based on the removal efficiencies of Cr(VI) (R-e, %) gotten in the single bioremediation system (default $\alpha = 0.05$)

Target	Source	Sum of squares (III)	df	Mean squares	F	Significance	Remarks
R-e	Corrected model	0.017	6	0.003	62.037	0.000	
	Intercept	6.910	1	6.910	154,273.931	0.000	
	C^a	0.007	3	0.002	49.173	0.000	$R^2 = 0.976$ (adjusted $R^2 = 0.961$)
	D^b	0.010	3	0.003	74.902	0.000	
	Error	0.000	9	4.479E-005			
	Total	6.927	16				
	Corrected total	0.017	15				

[a]Initial pH; [b]Ca^{2+} concentration (M).

have a significant influence on the removal of Cr(VI) from the aqueous environment in the single MICP experiments. The estimated marginal means became larger as each factor gradually reached higher levels. Summarily, the analytical results reflected that the initial over-alkali environment (i.e., pH is around 10) and the relatively high concentration of Ca^{2+} was beneficial to elevating the R-e values of Cr(VI) concerning the application of the MICP mechanism during the pure bioremediation process.

The fundamental elements dominating the bioremediation in the MICP mechanisms commonly include the mass transfer of urea to the bacteria, the production of the carbonate, and the adaptation of microorganisms to the toxic environment. The application of EK in the MICP

is to increase the effectiveness of mass transfer and adjust the aqueous acid-alkaline environment through the electrolysis of water (Eqs. (7) and (8)). The removal results of Cr(VI) (including both bacterial and bacteria-free groups, i.e., R-e and R-e$_{free}$) in the orthogonal tests describing the EK-MICP coupling system (i.e., bio-electrochemical system) are listed in Table 1. The significance-analysis results of the four variables are shown in Table 3 and the estimated marginal means governed by each factor are shown in Fig. 4b. The maximum R-e and R-e$_{free}$ were 97.63% and 36.78%, respectively, both achieved at the parametrical combination of voltage gradient of 1.5 V/cm (A4), remediation time of 12 d (B4), initial pH of 7 (C1), and the Ca^{2+}-concentration of 0.20 M (D4). The adjusted R^2 were 0.892

Table 3
Significance tests based on the removal efficiencies of Cr(VI) (R-e, R-e$_{free}$, %) gotten in the bio-electrochemical system

Target	Source	Sum of squares (III)	df	Mean squares	F	Significance	Remarks
R-e	Corrected model	0.230	12	0.019	11.322	0.035	
	Intercept	10.443	1	10.443	6,157.560	0.000	
	A^a	0.116	3	0.039	22.725	0.015	
	B^b	0.006	3	0.002	1.166	0.451	$R^2 = 0.978$ (Adjusted $R^2 = 0.892$)
	C^c	0.001	3	0.000	0.216	0.880	
	D^d	0.108	3	0.036	21.183	0.016	
	Error	0.005	3	0.002			
	Total	10.678	16				
	Corrected total	0.236	15				
R-e$_{free}$	Corrected model	0.145	12	0.012	35.022	0.007	
	Intercept	0.829	1	0.829	2,401.724	0.000	
	A^a	0.098	3	0.033	94.626	0.002	
	B^b	0.045	3	0.015	43.198	0.006	$R^2 = 0.993$ (adjusted $R^2 = 0.965$)
	C^c	0.002	3	0.001	1.615	0.352	
	D^d	0.001	3	0.000	0.650	0.634	
	Error	0.001	3	0.000			
	Total	0.976	16				
	Corrected total	0.146	15				

[a]Voltage gradient (V/cm); [b]remediation time (d); [c]initial pH; [d]Ca^{2+} concentration (M).

(for R-e) and 0.965 (for R-e$_{free}$), meaning the significance analysis based on the orthogonal experiments for the bio-electrochemical system was credible. The significance probabilities of four factors based on the R-e values were 0.015, 0.451, 0.880, and 0.016, respectively. The probabilities of four factors based on the R-e$_{free}$ values were 0.002, 0.006, 0.352, and 0.634, respectively. The significance results indicated that only the voltage gradient and Ca^{2+}-concentration among the four variables had a remarkable effect on the removal of Cr(VI) in the EK-MICP coupling system. Meanwhile, the voltage gradient and the remediation time have a more significant impact on the removal of Cr(VI) than the initial pH and the Ca^{2+}-concentration in the single EK system. The estimated marginal means based on R-e and R-e$_{free}$ (Fig. 4b) verified the significant results.

Overall, the changes in voltage gradients prominently affected the removal of Cr(VI) whether in the single EK process or the EK-MICP coupling system [30]. A relatively high voltage gradient guaranteed a positive result for the removal of Cr(VI) in electrokinetics. The effect of the remediation time (*B*) and initial pH (*C*) on the R-e values were not significant in the bio-electrochemical system (Table 3, R-e). The electrokinetics made MICP get rid of the high dependence on the bioremediation time and the initial over-alkali environment [20,31,32]. As shown in Fig. 4c, the grand mean of EK-MICP was larger than that of single EK or MICP, which directly demonstrated that the direct-electric field loaded over the medium enhanced the bioremediation of the *Bacillus* sp.H1 in terms of the removal of Cr(VI) from the stocking solution [32–34]. Considering the remarkable influence of the remediation time on the R-e$_{free}$ values in the EK process, the final optimization combination for the EK-MICP coupling system was determined as A$_4$B$_3$C$_3$D$_4$ (i.e., voltage gradient of 1.5 V/cm, the remediation time of 9 d, initial pH of 9, and the Ca^{2+}-concentration of 0.20 M) to obtain the maximum removal of Cr(VI) from the wastewater in the industrial application:

$$H_2O \rightarrow 2H^+ + \frac{1}{2}O_2(g) + 2e^- \tag{7}$$

$$2H_2O + 2e^- \rightarrow 2OH^- + H_2(g) \tag{8}$$

3.4. Kinetic simulation

The single MCIP and EK-MICP coupling experiments were conducted at the optimal conditions (i.e., B$_3$C$_3$D$_4$ for MICP, and A$_4$B$_3$C$_3$D$_4$ for EK-MICP) to obtain the raw data for the kinetic study. The kinetic fitting results for the bioremediation and bio-electrochemical system are shown in Fig. 5 and the corresponding kinetic parameters of the three models were calculated and listed in Table 4. The correlation coefficients (R^2) of the pseudo-first-order kinetic model for MICP and EK-MICP were 0.96674 and 0.98818, both closing to 1. However, the straight line fitted between t (horizontal axis) and $\ln(q_e - q_t)$ (vertical axis) were not quite suitable for the raw data of the EK-MICP, and the theoretical q_e had slightly deviated from the raw experimental value. The results indicated that the

pseudo-first-order kinetic model was appropriate for modeling the removal of Cr(VI) in the bioremediation while not apposite in the bio-electrochemical system. The R^2 values of the second-order kinetic model for MICP and EK-MICP were 0.83255 and 0.85516, respectively. The $q_{e,cal}$ values were both higher than the experimental values. The second-order kinetic model was not appropriate for the removal of Cr(VI) in both the two groups. The R^2 values of the Elovich model for MICP and EK-MICP were 0.99268 and 0.92797, separately. The straight line of $\ln(t)$ (horizontal axis) vs. q_t (vertical axis) for the bio-electrochemical system was more consistent with the raw data. The results demonstrated that the Elovich model was appropriate for modeling the removal of Cr(VI) in the bio-electrochemical system, while not suitable in the bioremediation. Generally, the fitting results demonstrated the effectiveness of electrokinetics on the removal of Cr(VI) in the bioremediation process from the perspective of kinetics.

3.5. Release characteristics of Cr(VI) from the precipitation

The immobilization of Cr(VI) in precipitations obtained from both the MICP and EK-MICP groups were analyzed using the five-stage Tessier sequential extraction method (Fig. S1) to evaluate the potential release characteristics of Cr(VI) from precipitations. The chemical speciation of Cr(VI) is shown in Fig. 6. The chromium in the precipitation was fractionated into five fractionations, including exchangeable, carbonate-bound, Fe–Mn oxides-bound, organic matter-bound, and residual fractions. As shown, the organic matter-bound fraction dominated the chemical speciation of Cr(VI) for both MICP and EK-MICP precipitations, and the corresponding percentages were 50.26% (for MICP) and 73.21% (for EK-MICP), respectively. The exchangeable fraction is the most active moiety among the five fractionations. The corresponding percentages were 40.12% (for MICP) and 22.34% (for EK-MICP), respectively. For Cr(VI) in the precipitation of EK-MICP, the exchangeable fraction was significantly reduced (i.e., from 40.12% to 22.34%), the total percentage of the Fe–Mn oxides-bound, organic matter-bound, and residual fractions was further compressed (Fig. 6), and the carbonate-bound fraction was contrarily increased (from 50.26% to 73.21%). Overall, the immobilization of Cr(IV) was enhanced in the EK-MICP coupling experiments compared with that in the single MICP.

4. Conclusion

The method of EK coupling MICP increased Cr(VI) removal from stocking solution more effectively compared with the single EK and pure MICP. *Bacillus* sp.H1 adapted well to the aqueous environment compensating with an up-limit of 80 g/L urea and 120 mg/L Cr(VI). The precipitation of Ca^{2+} changed in lockstep with the bacterial growth and the removal of Cr(VI) in the media with different Cr(VI) concentrations. Cr(VI) removal was mainly controlled by both the microbial bio-mineralization and the chemical precipitation of CaCrO$_4$. The initial over-alkali environment and relatively high concentration of Ca^{2+} facilitated the elevation of removal efficiencies of Cr(VI) in the pure MICP process. The voltage gradient and the

remediation time have a more significant impact on the removal of Cr(VI) than the other two factors in the single EK system. However, the voltage gradient and concentration of Ca^{2+} among the four variables played a more prominent role in affecting Cr(VI) removal in the EK-MICP coupling system. The optimization combination for the EK-MICP coupling system was finally determined, including the voltage gradient of 1.5 V/cm, the remediation time of 9 d, the initial pH of 9, and Ca^{2+} concentration of 0.20 M. The pseudo-first-order kinetic model was appropriate for modeling Cr(VI) removal in bioremediation. Contrarily, the Elovich

model was preferably selected to model Cr(VI) removal in the bio-electrochemical system. The immobilization of Cr(IV) in the precipitation was strengthened in the EK-MICP coupling experiments compared with that in the pure MICP.

Data availability statement

All data, models, or code generated or used during the study are available from the corresponding author by requests, such as the original experimental data, the biological characteristics including bacterial growth, urease
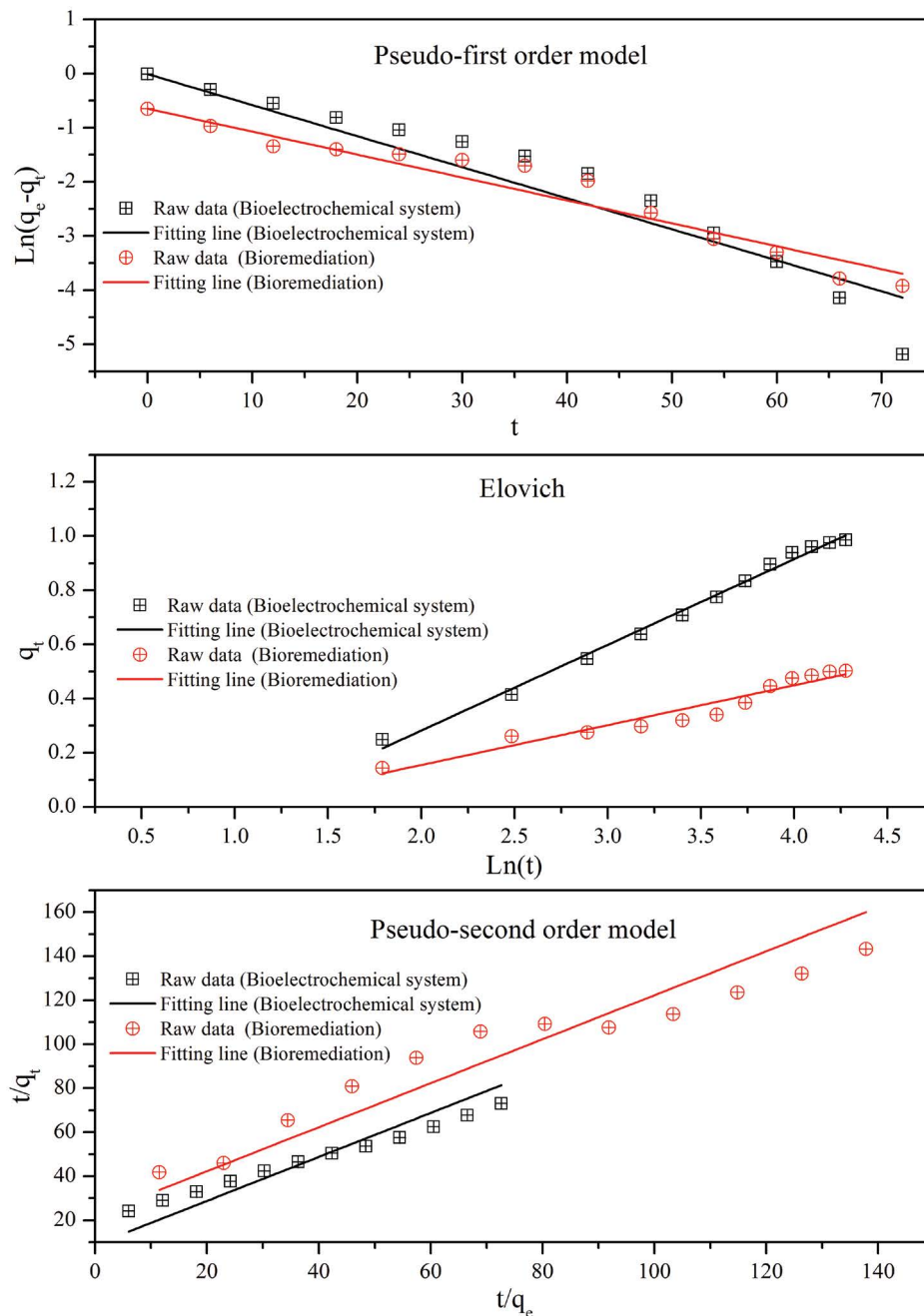
Fig. 5. Kinetic fitting results under the optimal condition for the bioremediation and bio-electrochemical system.

Table 4
Kinetic parameters of three models in the bioremediation and bio-electrochemical system

Models	Parameters	Bio-electrochemical system (EK-MCIP)	Bioremediation (MICP)
First-order-kinetic model:	k_1	0.05732	0.04231
$\ln\left(q_e - q_t\right) = \ln q_e - k_1 t$	R^2	0.96674	0.98818
	$q_{e,\mathrm{cal}}$	1.00176	0.52768
Second-order-kinetic model:	k_2	0.09109	0.12690
$\dfrac{t}{q_t} = \dfrac{1}{k_2 q_e^2} + \dfrac{t}{q_e}$	R^2	0.83255	0.85516
	$q_{e,\mathrm{cal}}$	1.11980	0.59504
Elovich:	a	0.10439	0.05700
	b	3.15896	6.79486
$q_t = \dfrac{1}{b}\ln\left(ab\right) + \dfrac{1}{b}\ln\left(t\right)$	R^2	0.99268	0.92797

k_1 is the pseudo first-order rate constant (min^{-1}); k_2 is the pseudo-second-order rate constant (g/mg min); q_e represents the adsorption capacity (mg/g) of Cr(VI) at the equilibrated moment (h), q_t is the adsorption capacity (mg/g) of Cr(VI) at t moment (h).
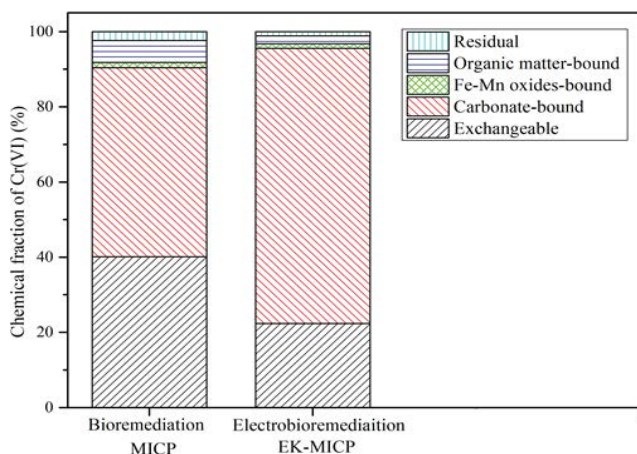

Fig. 6. Chemical fractionation of Cr(VI) in the precipitations obtained from bioremediation and bio-electrochemical system.

production, and ureolytic activity of the isolated bacterial, the design of an orthogonal test, the kinetic model constructed in the study, a five-step sequential extraction procedure, etc.

Acknowledgments

References

[1] T. Huang, L.F. Liu, L.L. Zhou, S.W. Zhang, Electrokinetic removal of chromium from chromite ore-processing residue using graphite particle-supported nanoscale zero-valent iron as the three-dimensional electrode, Chem. Eng. J., 350 (2018) 1022–1034.

[2] M.S. Samuel, J. Bhattacharya, S. Raj, N. Santhanam, H. Singh, N.D.P. Singh, Efficient removal of chromium(VI) from aqueous solution using chitosan grafted graphene oxide (CS-GO) nanocomposite, Int. J. Biol. Macromol., 121 (2019) 285–292.

[3] C.G. Gao, X.L. Zhang, Y. Yuan, Y. Lei, J.T. Gao, S.J. Zhao, C.Y. He, L.C. Deng, Removal of hexavalent chromium ions by core-shell sand/Mg-layer double hydroxides (LDHs) in constructed rapid infiltration system, Ecotoxicol. Environ. Saf., 166 (2018) 285–293.

[4] J.E. Rager, M. Suh, G.A. Chappell, C.M. Thompson, D.M. Proctor, Review of transcriptomic responses to hexavalent chromium exposure in lung cells supports a role of epigenetic mediators in carcinogenesis, Toxicol. Lett., 305 (2019) 40–50.

[5] W.L. Li, X.X. Xue, Effects of boron oxide addition on chromium distribution and emission of hexavalent chromium in stainless-steel slag, Ind. Eng. Chem. Res., 57 (2018) 4731–4742.

[6] L.H. Nguyen, T.M.P. Nguyen, H.T. Van, X.H. Vu, T.L.A. Ha, T.H.V. Nguyen, X.H. Nguyen, X.C. Nguyen, Treatment of hexavalent chromium contaminated wastewater using activated carbon derived from coconut shell loaded by silver nanoparticles: batch experiment, Water Air Soil Pollut., 230 (2019), doi: 10.1007/s11270-019-4119-8.

[7] D. Pradhan, L.B. Sukla, B.B. Mishra, N. Devi, Biosorption for removal of hexavalent chromium using microalgae *Scenedesmus* sp., J. Cleaner Prod., 209 (2019) 617–629.

[8] K. Rhoades, J. Eun, J.M. Tinjum, Transport of hexavalent chromium in the vadose zone by capillary and evaporative transport from chromium ore processing residue, Can. Geotech. J., 53 (2016) 619–633.

[9] J.A. Korak, R.G. Huggins, M.S. Arias-Paic, Nanofiltration to improve process efficiency of hexavalent chromium treatment using ion exchange, J. Am. Water Works Assoc., 110 (2018) E13–E26.

[10] W.Y. Duan, G.D. Chen, C.X. Chen, R. Sanghvi, A. Iddya, S. Walker, H.Z. Liu, A. Ronen, D. Jassby, Electrochemical removal of hexavalent chromium using electrically conducting carbon nanotube/polymer composite ultrafiltration membranes, J. Membr. Sci., 531 (2017) 160–171.

[11] A. Saravanan, P.S. Kumar, M. Yashwanthraj, Sequestration of toxic Cr(VI) ions from industrial wastewater using waste biomass: a review, Desal. Water Treat., 68 (2017) 245–266.

[12] H.P. Luo, H. Li, Y.B. Lu, G.L. Liu, R.D. Zhang, Treatment of reverse osmosis concentrate using microbial electrolysis desalination and chemical production cell, Desalination, 408 (2017) 52–59.

[13] E. Leiva, E. Leiva-Aravena, C. Rodriguez, J. Serrano, I. Vargas, Arsenic removal mediated by acidic pH neutralization and iron precipitation in microbial fuel cells, Sci. Total Environ., 645 (2018) 471–481.

[14] R. Jobby, P. Jha, A.K. Yadav, N. Desai, Biosorption and biotransformation of hexavalent chromium [Cr(VI)]: a comprehensive review, Chemosphere, 207 (2018) 255–266.

[15] K.K. Raj, U.R. Sardar, E. Bhargavi, I. Devi, B. Bhunia, O.N. Tiwari, Advances in exopolysaccharides based bioremediation of

heavy metals in soil and water: a critical review, Carbohydr. Polym., 199 (2018) 353–364.

[16] Y. Yang, T.H. Chen, M. Sumona, B. Sen Gupta, Y.B. Sun, Z.H. Hu, X.M. Zhan, Utilization of iron sulfides for wastewater treatment: a critical review, Rev. Environ. Sci. Biotechnol., 16 (2017) 289–308.

[17] A.K. Zeraatkar, H. Ahmadzadeh, A.F. Talebi, N.R. Moheimani, M.P. McHenry, Potential use of algae for heavy metal bioremediation, a critical review, J. Environ. Manage., 181 (2016) 817–831.

[18] S. Bibi, A. Hussain, M. Hamayun, H. Rahman, A. Iqbal, M. Shah, M. Irshad, M. Qasim, B. Islam, Bioremediation of hexavalent chromium by endophytic fungi; safe and improved production of *Lactuca sativa* L., Chemosphere, 211 (2018) 653–663.

[19] A.J. Phillips, E. Troyer, R. Hiebert, C. Kirkland, R. Gerlach, A.B. Cunningham, L. Spangler, J. Kirksey, W. Rowe, R. Esposito, Enhancing wellbore cement integrity with microbially induced calcite precipitation (MICP): a field scale demonstration, J. Pet. Sci. Eng., 171 (2018) 1141–1148.

[20] A.E. Torres-Aravena, C. Duarte-Nass, L. Azocar, R. Mella-Herrera, M. Rivas, D. Jeison, Can microbially induced calcite precipitation (MICP) through a ureolytic pathway be successfully applied for removing heavy metals from wastewaters?, Crystals, 8 (2018), doi: 10.3390/cryst8110438.

[21] Y. Al-Salloum, S. Hadi, H. Abbas, T. Almusallam, M.A. Moslem, Bio-induction and bioremediation of cementitious composites using microbial mineral precipitation - a review, Constr. Build. Mater., 154 (2017) 857–876.

[22] D. Mujah, M.A. Shahin, L. Cheng, State-of-the-art review of biocementation by microbially induced calcite precipitation (MICP) for soil stabilization, Geomicrobiol. J., 34 (2017) 524–537.

[23] T. Huang, L.F. Liu, S.W. Zhang, Electrokinetic enhancement: effect of sample stacking on strengthening heavy metal removal in electrokinetic remediation of municipal solid waste incineration fly ash, J. Environ. Eng., 145 (2019), doi: 10.1061/(ASCE)EE.1943-7870.0001501.

[24] T. Huang, S.W. Zhang, L.F. Liu, Immobilization of trace heavy metals in the electrokinetics-processed municipal solid waste incineration fly ashes and its characterizations and mechanisms, J. Environ. Manage., 232 (2019) 207–218.

[25] T. Huang, L.F. Liu, S.W. Zhang, J.J. Xu, Evaluation of electrokinetics coupled with a reactive barrier of activated carbon loaded with a nanoscale zero-valent iron for selenite removal from contaminated soils, J. Hazard. Mater., 368 (2019) 104–114.

[26] Z. Hurak, F. Foret, On benchmark problems, challenges, and competitions in electrokinetics - a review, Electrophoresis, 36 (2015) 1429–1431.

[27] Y.L. Liu, J. Zhang, H.J. He, Assessment of the Tessier and BCR sequential extraction procedures for elemental partitioning of Ca, Fe, Mn, Al, and Ti and their application to surface sediments from Chinese continental shelf, Acta Oceanol. Sin., 37 (2018) 22–28.

[28] D. Rosado, J. Usero, J. Morillo, Ability of 3 extraction methods (BCR, Tessier and protease K) to estimate bioavailable metals in sediments from Huelva estuary (Southwestern Spain), Mar. Pollut. Bull., 102 (2016) 65–71.

[29] L.M. Lun, D.W. Li, Y.J. Yin, D. Li, G.J. Xu, Z.Q. Zhao, S. Li, Characterization of chromium waste form based on biocementation by *Microbacterium* sp GM-1, Indian J. Microbiol., 56 (2016) 353–360.

[30] T. Huang, S.W. Zhang, L.F. Liu, J.J. Xu, Graphite particle electrodes that enhance the detoxification of municipal solid waste incineration fly ashes in a three-dimensional electrokinetic platform and its mechanisms, Environ. Pollut., 243 (2018) 929–939.

[31] E.Z. Gomaa, Biosequestration of heavy metals by microbially induced calcite precipitation of ureolytic bacteria, Rom. Biotechnol. Lett., 24 (2019) 147–153.

[32] K.M. Darby, G.L. Hernandez, J.T. DeJong, R.W. Boulanger, M.G. Gomez, D.W. Wilson, Centrifuge model testing of liquefaction mitigation via microbially induced calcite precipitation, J. Geotech. Geoenviron. Eng., 145 (2019), doi: 10.1061/9780784481455.012.

[33] M. Oualha, S. Bibi, M. Sulaiman, N. Zouari, Microbially induced calcite precipitation in calcareous soils by endogenous *Bacillus cereus*, at high pH and harsh weather, J. Environ. Manage., 257 (2020), doi: 10.1016/j.jenvman.2019.109965.

[34] A. Mahawish, A. Bouazza, W.P. Gates, Improvement of coarse sand engineering properties by microbially induced calcite precipitation, Geomicrobiol. J., 35 (2018) 887–897.

Supporting information

S1. Chemicals and reagents

Hydrochloric acid (HCl, 30%) and sodium hydroxide (NaOH, ACS, 97%) were purchased from HUAFU Chemical Co., Ltd., (Yangzhou, China) for the adjustment of the initial pH in medium and stocking solution. The peptone, tryptone, yeast extract (Powder, BR), and beef extract (BR) were got from Shanghai Macklin Biochemical Co., Ltd., (Shanghai, China). The sodium chloride (NaCl, 99.99%, metal basis), potassium phosphate monobasic (KH_2PO_4, 99%), urea (CH_4N_2O, 99.5%), glucose monohydrate (USP, $C_6H_{12}O_6 \cdot H_2O$) were obtained from Aladdin for the preparation of Urease-selective (URS) medium, Luria–Bertani (LB) medium and Nutrient Broth (NB) medium. The specifications of the three media were detailed in the supporting information (Tables S1–S3). Phenolsulfonphthalein ($C_{19}H_{14}O_5S$) was bought from GUI DE CHEM (Wuhan, China) to indicate the existence of urease. All the chemicals and reagents were sterilized before the usage.

S2. Isolation and activation of ureolytic bacteria

The NB medium (100 mL) added with 50 g/L urea, 50 µmol/L Ni^{2+}, 0.05 M $CaCl_2$, and 90–150 mg/L $K_2Cr_2O_7$ were prepared and sterilized for MICP experiments. 10 mL of *Bacillus* sp.H1 at the logarithmic stage was inoculated into the medium, and shaken over 4 d at the constant temperature of 25°C. The initial pH was adjusted to eight before the inoculation procedure. The changes in calcite precipitation and removal efficiency (R-e, %) over the MICP experiments were monitored to evaluate the performance of the bacterially induced calcite-precipitation. A hundred microliters of bacterial inoculation were transferred to a conical flask containing LB medium (Tables S2) using a small-range pipettor and shaken in a thermostatic oscillating shaker (SHZ-B, KEMAI, China) to re-active the metabolism of *Bacillus* sp.H1. To test the urease activity, *Bacillus* sp.H1 was dipped using a metal loop and draw on the plate of the URS medium following the zig lines. The plate was inverted and marked, and incubated in an incubator (SHH-01D, JIANHENG INSTRUMENT Co., Ltd., China) for 2 d. A urea-free group was set as the control run. 2 mL *Bacillus* sp.H1 solution was added to Erlenmeyer flasks containing the NB medium (Table S3), and shaken at 150 rpm until the liquid began to become turbid. A microplate reader was periodically used to measure the concentration of urease at intervals of 3 h, which also directly reflected the bacterial growth. The detection wavelength is adjusted at 600 nm, and the recorded results were labeled as OD_{600} (i.e., indicating the concentration of urease). The urea solution was injected into 100 mL NB medium after

the filtration and sterilization. The final urea concentration in the medium is 40, 60, 80, 100, and 120 g/L, respectively. 10 mL of *Bacillus* sp.H1 at the logarithmic stage was added to the urea-containing medium to evaluate the bacterial tolerance ceiling. The NB medium supplemented with 30, 60, 90, 120, 150, and 180 mg/L $K_2Cr_2O_7$ was used to measure the bacterial resistance against Cr(VI). The aforementioned experiments were all conducted in triplicate.

S3. Equations

Three known kinetic models including the pseudo-first-order model, pseudo-second-order model, and Elovich were modified to simulate the removal process of Cr(VI) in the bioremediation and bio-electrochemical experiments. The removal capacities at equilibrated and t moment (i.e., q_e and q_t) were substituted by the removal efficiencies of Cr(VI) at a specific time. Thus, q_e and q_t correspondingly represent the removal efficiencies of Cr(VI) at equilibrated and t moment (h), respectively in terms of the Eqs. ((S1)–(S3)), k_1, k_2, a and b are the rate constants to be sequentially calculated.

Pseudo-first-order model:

$$\ln\left(q_e - q_t\right) = \ln q_e - k_1 t \tag{S1}$$

Pseudo-second-order model:

$$\frac{t}{q_t} = \frac{1}{k_2 q_e^2} + \frac{t}{q_e} \tag{S2}$$

Elovich:

$$q_t = \frac{1}{b}\ln\left(ab\right) + \frac{1}{b}\ln\left(t\right) \tag{S3}$$

Table S1
Urease-selective medium

Peptone	NaCl	KH$_2$PO$_4$	CH$_4$N$_2$O	C$_6$H$_{12}$O$_6$·H$_2$O	C$_{19}$H$_{14}$O$_5$S
1 g/L	5 g/L	2 g/L	2 g/L	0.1 g/L	0.2%

Table S2
Luria–Bertani medium

Tryptone	Yeast extract	NaCl
10 g/L	5 g/L	10 g/L

Table S3
Nutrient Broth medium

Peptone	Beef extract	NaCl
10 g/L	3 g/L	5 g/L

Table S4
Four factors at four different levels in the orthogonal tests (V_0)

Level	A: Voltage gradient (V/cm)	B: Remediation time (d)	C: Initial pH	D: Ca^{2+} concentration (M)
1	0.1	3	7	0.05
2	0.5	6	8	0.10
3	1.0	9	9	0.15
4	1.5	12	10	0.20

Table S5
Design of two-factor experiments based on the Cr(VI) removal efficiencies (R-e) for the bioremediation process (at the remediation time of 9 d and voltage gradient of 0 V/cm)

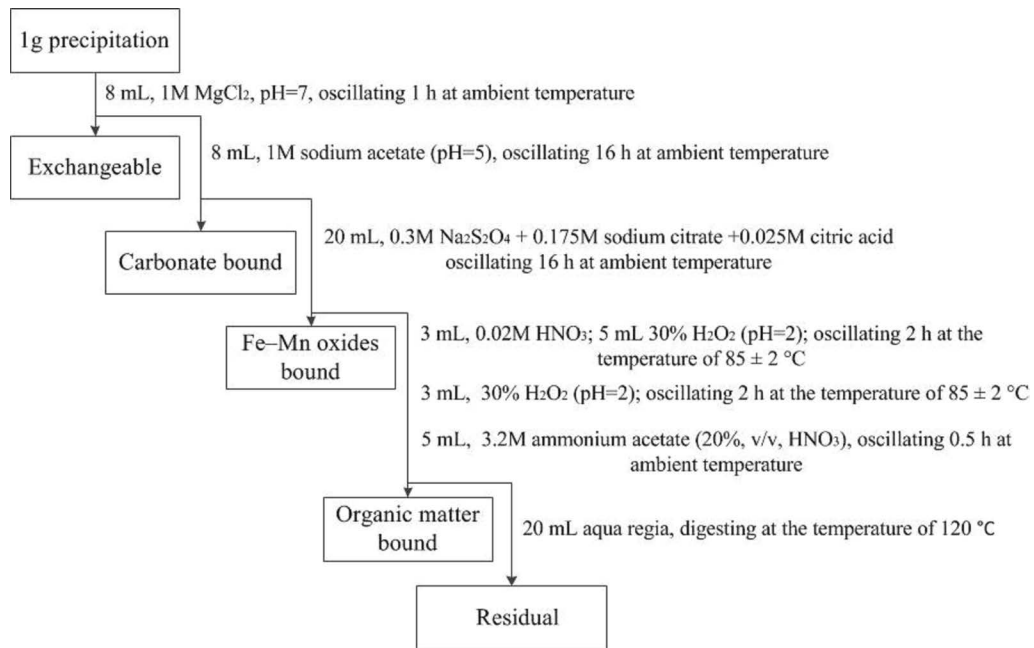| R-e		C[a]			
		1 (7)	2 (8)	3 (9)	4 (10)
D[b]	1 (0.05 M)	60.75%	61.28%	62.94%	65.09%
	2 (0.10 M)	62.24%	63.05%	64.52%	67.78%
	3 (0.15 M)	64.81%	65.57%	67.79%	68.87%
	4 (0.20 M)	66.37%	67.15%	69.89%	73.36%

[a]initial pH; [b]Ca^{2+} concentration (M).

Fig. S1. Five-stage Tessier sequential extraction of Cr(VI).